A Simple Line-Frequency Commutation Cell Improving Power Factor and Voltage Regulation of Rectifiers with Passive L-C Filter

Giorgio Spiazzi
Department of Electronics and Informatics, University of Padova
Via Gradenigo 6A - 35131 Padova - ITALY
Tel. (+39-049) 827-7525 - Fax (+39-049) 827-7699
e-mail: spiazzi@dei.unipd.it

Eduardo da Silva Martins, José Antenor Pomilio
School of Electrical and Computer Engineering, University of Campinas
C. P. 6101 13081-970 Campinas – BRAZIL
Tel. (+55-19) 7883748 – Fax (+55-19) 2891395
e-mail: antenor@dsce.fee.unicamp.br

Abstract. **The paper presents a simple cell with a line-frequency commutated AC switch that is able to greatly improve both power factor and output voltage regulation of rectifiers with passive L-C filters. The boost action introduced by the commutation cell allows for the compensation of the voltage drop across the input filter inductor, so as output voltages higher than the peak of the line voltage can be achieved. Moreover, as compared to the line-frequency commutated boost rectifier, the proposed circuit allows compliance with the low-frequency harmonic standard EN 61000-3-2 with a lower filter inductance value, at output power levels greater than 1kW. A converter prototype was built and tested. Results are reported in order to confirm the theoretical analysis.**

I. INTRODUCTION

High frequency power factor correctors (PFCs) providing very high power factors as well as good output voltage regulation are increasingly substituting conventional front-end rectifiers due to harmonic limits imposed by international standards like EN-61000-3-2 [1]. The penalty of such improvement in the absorbed line current is an increase of the overall ac-to-dc converter size and cost, sometimes not justified in large volume applications like household appliances, TV sets etc. In such cases, standard low-cost high-reliable rectifiers with passive filters are still used in order to improve the quality of the current drawn from the line, even if the volume of the reactive components needed becomes rapidly prohibitive as the power increases [2].

Several line frequency commutated rectifier topologies have been presented in literature as a trade off between cost and performances [3-6]. All of them provide compliance with the standards with a lower reactive component volume, as compared with passive L-C filters, by increasing the input current conduction angle through the use of a line-frequency commutated switch, plus other few components.

The same principle is exploited in the proposed line-frequency commutation cell, which has the following advantages:

- possibility to be used in existing rectifiers with passive L-C filters;
- high power factor as compared to standard L-C rectifiers;
- inherent switch short circuit protection;
- possibility to achieve output voltage regulation in wide line and load variation ranges;
- lower inductor value needed to comply with IEC 61000-3-2 standard as compared to the line-frequency commutated boost rectifier [3,4].

The operation principles of the proposed rectifier are explained in the paper and different design procedures are suggested.

Measurements made on a converter prototype showed a good agreement with the theoretical expectations.

II. PRINCIPLE OF OPERATION

A single-phase rectifier with passive L-C_L filter is shown in Fig. 1 together with the proposed line-frequency commutation cell composed by AC switch S and capacitors C_1 and C_2. The cell operation is described in the following with the help of Fig. 2, which reports input current i_g and voltage u_2 waveforms in the first line half period, in which voltage u_g is positive, together with the switch gate drive signal. As we can see, two different situations can occur, depending on the capacitor initial voltage U_{20}, as illustrated in Figs. 2a), where $U_{20} = 0$ and 2b), where $U_{20} \neq 0$. Expressions for the input current i_g and resonant capacitor voltage u_2 are reported in Table I in normalized form by using the following base quantities and definitions:

Line voltage: ..... $u_g(\theta) = U_{pk}\sin(\theta),\ \theta = \omega_i t$

Base voltage: ..... $U_N = U_{pk}$ (1.a)

Base current: ..... $I_N = \dfrac{U_{pk}}{\omega_i L}$ (1.b)

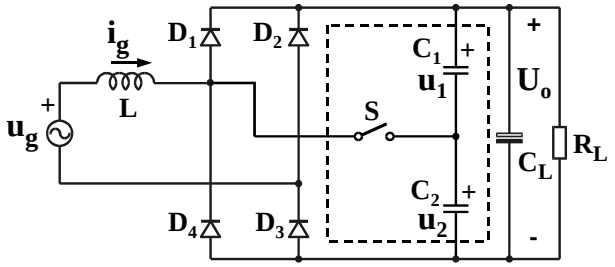

Fig.1 – Scheme of a rectifier with passive L-C_L filter with the proposed line-frequency commutation cell (S is an AC switch)

Resonant angular frequency:..... $\omega_o = \dfrac{1}{\sqrt{2LC}}$ (1.c)

Normalized resonance frequency:.. $\alpha = \dfrac{\omega_o}{\omega_i}$ (1.d)

Voltage conversion ratio:..... $M = \dfrac{U_o}{U_{pk}}$ (1.e)

For the analysis, the output voltage ripple was neglected, so that U_o is considered constant.

A) Resonant interval $\theta_1 < \theta < \theta_2$.

The switch S is turned on, by the control circuit, with a constant delay T_d with respect to the line voltage zero crossing: if the initial capacitor voltage U_{20} is zero or, anyway, lower than the input voltage at this instant, the resonance cycle between the input inductor L and the equivalent capacitor $C_1+C_2 = 2C$ ($C_1 = C_2 = C$) starts (these are the cases considered in Figs. 2a) and b)). In this case, the initial instant θ_1 in which the input current starts to flow coincides with θ_d. On the other hand, if at instant θ_d the input voltage is lower than the initial capacitor voltage U_2, then the input current starts to flow only when diode D_3 becomes forward biased, so that $\theta_1 > \theta_d$. In summary, we can write:

$$\theta_1 = \max\left\{\theta_d, \sin^{-1}\left(U_{20N}\right)\right\} \quad (2)$$

During the resonant interval the input current divides almost equally ($C_L >> C_1,C_2$) between C_1 and C_2 and returns through diode D_3. The equations describing normalized input current and capacitor voltage during this phase are reported in Table I. This interval can be terminated either by the switch turn-off (if U_{20} was greater than zero as shown in Fig. 2b) or by turn-on of diode D_1 (if U_{20} was zero as shown in Fig. 2a), which occurs when voltage u_2 becomes equal to the output voltage U_o (the case in which the input current zeroes after a half resonant cycle is not considered since it gives rise to a high input current distortion, and must be avoided by a proper design). In the first case, the final voltage across capacitor C_2, at steady state, must be equal to U_o-U_{20}. This condition can be exploited in order to calculate the initial capacitor voltage U_{20} by using the equation in the last row of Table I. Such equation can be solved directly only in the case $\theta_1 = \theta_d$ since the conduction angle θ_c coincides with the switch on-time, and is therefore imposed by the control (it is a known quantity in the formula). In the other case, such equation must be solved numerically since θ_c becomes a function of U_{20} ($\theta_c = \theta_2 - \theta_1 = \theta_{on} - \sin^{-1}\left(U_{20N}\right) + \theta_d$ and θ_{on} corresponds to the switch on interval)

B) Discharging interval $\theta_2 < \theta < \theta_3$.

At the end of the previous phase, the capacitor voltage u_2 is either U_o or U_o-U_{20} and the inductor energy discharges to the output filter capacitor and to the load through diodes D_1 and D_3. The equation describing its behavior is reported in Table I, where I_{g0} is the inductor current value at the end of the resonant interval. When the current goes to zero, the diodes turn-off and the energy to the load is delivered only by the output capacitor.

During the input voltage negative half cycle, the operations remain the same with a negative input current and with voltage u_1 considered instead of u_2.

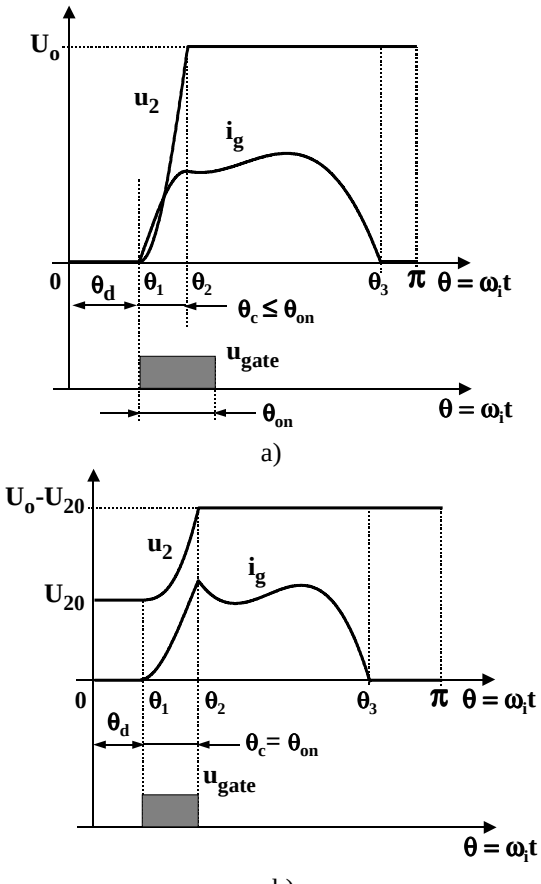

Fig.2 – Input current i_g and capacitor voltage u_2 in the first line half period. a) Initial capacitor voltage $U_{20} = 0$; b) initial capacitor voltage $U_{20} > 0$ and $U_{pk} \sin(\theta_d) > U_{20}$ ($\theta_1 = \theta_d$)

TABLE I - EQUATIONS DESCRIBING NORMALIZED INPUT CURRENT I_{gN} AND CAPACITOR VOLTAGE U_{2N} IN A LINE HALF PERIOD

Intervals	Fundamental equations
$0 \le \theta \le \theta_1$	$i_{gN}(\theta)=0\ ,\ u_{2N}(\theta)=U_{20N}$
$\theta_1 \le \theta \le \theta_2$	$i_{gN}(\theta)=\frac{\cos(\theta_1)}{\alpha^2-1}[\cos(\theta-\theta_1)-\cos(\alpha(\theta-\theta_1))]-\frac{\sin(\theta_1)}{\alpha^2-1}[\sin(\theta-\theta_1)-\alpha\sin(\alpha(\theta-\theta_1))]-\frac{U_{20N}}{\alpha}\sin(\alpha(\theta-\theta_1))$ $u_{2N}(\theta)=U_{20N}\cos(\alpha(\theta-\theta_1))+\frac{\alpha^2}{\alpha^2-1}\left[\cos(\theta_1)\left[\sin(\theta-\theta_1)-\frac{1}{\alpha}\sin(\alpha(\theta-\theta_1))\right]+\sin(\theta_1)[\cos(\theta-\theta_1)-\cos(\alpha(\theta-\theta_1))]\right]$ $I_{g0N}=i_{gN}(\theta_2)$
$\theta_2 \le \theta \le \theta_3$	$i_{gN}(\theta)=I_{g0N}+\cos(\theta_2)-\cos(\theta)-M(\theta-\theta_2)$ $u_{2N}(\theta)=M-U_{20N}$
$\theta_3 \le \theta \le \pi$	$i_{gN}(\theta)=0\ ,\ u_{2N}(\theta)=M-U_{20N}$
$U_{20N}=\frac{1}{1+\cos(\alpha\theta_c)}\left\{M-\frac{\alpha^2}{\alpha^2-1}\left[\cos(\theta_1)\left[\sin(\theta_c)-\frac{1}{\alpha}\sin(\alpha\theta_c)\right]+\sin(\theta_1)[\cos(\theta_c)-\cos(\alpha\theta_c)]\right]\right\}$	

As we can see, in the case ($U_{20} = 0$) the resonant interval θ_c depends only on the resonant circuit parameters L and C and on the delay interval θ_d, while in the other cases it depends also on the switch on interval θ_{on}. Anyway, like other line-frequency commutated rectifiers [3-6], the resonance phase causes a strong boost action, which can easily compensate for the inductor voltage drop. Moreover, the normalized resonance frequency α gives another degree of freedom in the converter design, as compared to the standard boost rectifier [3,4], which helps to obtain a satisfactory (in terms of harmonic content) input current waveform, with a reduced cost and volume.

III. DESIGN EXAMPLES

Similarly to other line-frequency commutated rectifiers, there are many parameters (inductor value, resonance frequency, delay and turn-on times) that influence, in a complex way, the input current waveform and the output voltage and power. Thus, different design approaches can be developed, depending on the desired goal. In the following, two different design examples are illustrated in order to show the converter potentiality.

A) Design for Maximum Voltage Regulation Range

In this design example, the goal is to maintain a constant output voltage irrespective of line and load variations. In order to do that, the input inductor and the resonant capacitor values are calculated so as to ensure a non zero input current in the whole line period at the minimum input voltage and for the desired output voltage and power, assuming the switch is always kept on. Then, compliance with EN 61000-3-2 standard is tested at $U_g = 230\ V_{RMS}$, as required by the norm: if it fails, a lower output voltage or a reduced input voltage range must be used. Considering a non zero input current in the whole line period, allows to derived a closed loop design procedure as illustrated hereafter. By letting $\theta_1 = \theta_d = 0$ and $U_{20} = 0$, the input current i_g and capacitor voltage u_2 equations reduce to:

$$i_{gN}(\theta)=\frac{1}{\alpha^2-1}[\cos(\theta)-\cos(\alpha\theta)] \tag{3}$$

$$u_{2N}(\theta)=\frac{\alpha^2}{\alpha^2-1}\left[\sin(\theta)-\frac{1}{\alpha}\sin(\alpha\theta)\right] \tag{4}$$

The conduction angle θ_c is determined by the instant in which u_2 reaches the output voltage value, i.e. from (4):

$$u_{2N}(\theta_c)=M_{max}=\frac{\alpha^2}{\alpha^2-1}\left[\sin(\theta_c)-\frac{1}{\alpha}\sin(\alpha\theta_c)\right] \tag{5}$$

where the maximum desired voltage conversion ratio $M_{max} = U_o/U_{pkmin}$ is used. Then, the input current evolves as prescribed by the corresponding equation in Table I, where, in this case, $\theta_2 = \theta_c$. From this equation, by imposing $\theta_3 = \pi$, the following constraint can be derived (I_{g0N} is derived by letting $\theta = \theta_c$ in (3)):

$$\frac{1}{\alpha^2-1}\left[\alpha^2\cos(\theta_c)-\cos(\alpha\theta_c)\right]+1-M_{max}(\pi-\theta_c)=0 \tag{6}$$

Eqs. (5) and (6) can be solved together (in a numerical way) in order to find α and θ_c. Then, from the input current waveform, the input power is calculated as follows:

$$\begin{aligned} P_{in} &= \frac{1}{\pi}\int_0^{\pi} u_g(\theta)i_g(\theta)\,d\theta = \\ &= \frac{U_{pk}^2}{\omega_i L}\frac{1}{\pi}\int_0^{\pi} u_{aN}(\theta)i_{aN}(\theta)\,d\theta = \frac{U_{pk}^2}{\omega_i L}P_{inN} \end{aligned} \tag{7}$$

where P_{inN} is the normalized input power, and the inductor value is calculated from (7) based on the desired input power. Finally, from the definition of the normalized resonance frequency α, the value of resonant capacitor C_1 and C_2 is calculated. Fig. 3 reports the normalized input

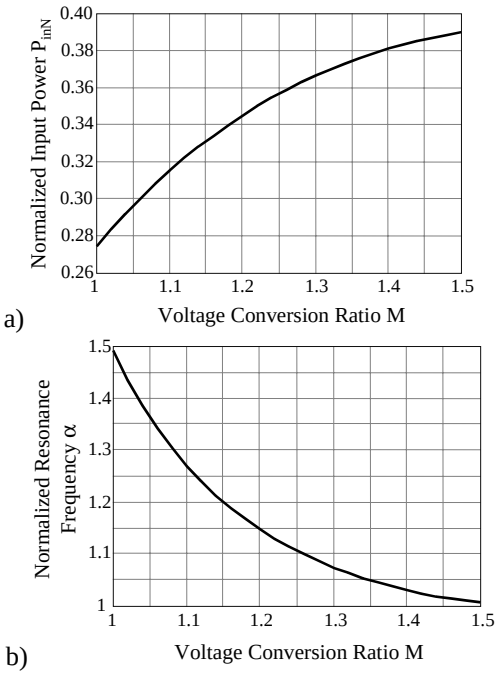

Fig. 3 – Normalized input Power P_{inN} (a) and resonance frequency α (b) as a function of the voltage conversion ratio M in the case of a non zero input current in the whole line period ($\theta_3 = \pi$)

power P_{inN} and resonance frequency α as a function of the voltage conversion ratio M, which can be used in the outlined design procedure.

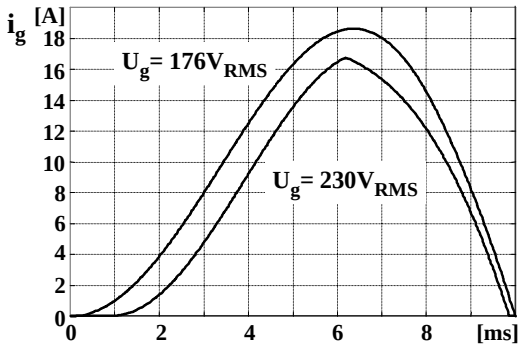

Fig. 4 – Input current waveform at two different input voltage values (P_{in} = 2kW, U_o = 350 V)

As an example, let us consider the following specifications:

Input voltage: $U_g = 176 \div 264\ V_{RMS}$,
Input power: P_{in} = 2kW,
Output voltage: U_o = 350 V

The outlined design procedure yields the following parameter values: L = 37.6mH, and $C_1 = C_2$ = 127 μF.

The simulated input current waveform is shown in Fig. 4 for U_g = 176 V_{RMS} and U_g = 230 V_{RMS}: in the latter case, the input current peak value is 16.26 A, the fundamental current amplitude is 13.1 A, the cos(ϕ) is 0.94 and the power factor is 0.91. In order to maintain the same output voltage value, the switch on-time was reduced to 6.1ms ($\theta_d = 0$).

With the chosen output voltage value, at the maximum input voltage the regulation is lost below 3% of the nominal load. Below U_g = 247 V_{RMS}, a complete output voltage regulation from no load to full load is achieved.

For the purpose of comparison, a simple L-C_L filter, at the same output power, complies with the standard with 28mH of input inductor, peak current value of 20.19 A, cos(ϕ) of 0.695, and power factor of 0.682. The resulting output voltage is 188V, at 230 V_{RMS} input voltage.

B) Design for Compliance with Standards.

If the goal is to comply with the standard without care for the output voltage regulation at different input voltage values, the needed inductor value can be significantly reduced. Considering the previous example, compliance with the standard can be achieved with L = 17.2mH, $C_1 = C_2$ = 45.4 μF, (T_d = 0s, T_{ON} = 4ms, I_{g_pk} = 15.32 A, I_1 = 12.66 A, cos(ϕ) = 0.973, PF = 0.943). Clearly, the capability of voltage regulation against load variations is maintained, while it is lost for input voltage variations. For the purpose of comparison, a line-frequency commutated boost [3,4] needs an inductor value of 22mH in order to comply with the standard, at U_o = 298.5 V (T_d = 0s, T_{ON} = 2.35ms, I_{g_pk} = 12.15 A, I_1 = 12.29 A, cos(ϕ) = 0.99, PF = 0.986).

IV. Experimental Results

A 2 kW prototype was built and tested. The following parameters were calculated using the approach for maximum output voltage regulation:

$U_g = 176 \div 264\ V_{RMS}$
L = 31 mH (available at the laboratory)
$C_1 = C_2$ = 126 μF
C_L = 940 μF

The resulting waveforms are shown in Fig. 5. The switch command signal is high during all the time for U_g = 176V_{RMS}. The current through the auxiliary switch stops when the auxiliary capacitor current zeroes. The resulting power factor is 0.97. The output voltage is regulated in 303V, lower than expected due to converter losses. The measured efficiency is 91%.

For U_g = 220V_{RMS} the auxiliary switch changes the duty-cycle, altering the input current shape but maintaining the output voltage constant. For this situation the input voltage and current waveforms are shown in Fig. 6. The measured efficiency has increased to 93 % due to the lower current value. The power factor is 0.95. The current spectrum is shown in Fig. 7 and Table II indicates the measured harmonic amplitudes, compared with Class A limits.

For the maximum input voltage, the input voltage and current waveforms are shown in Fig. 8. The output Voltage is 302 V, the efficiency is 95 % and the power factor is 0.93.

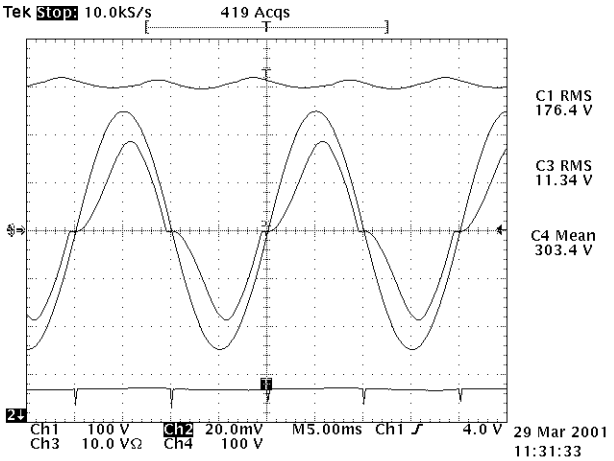

Fig. 5 – Waveforms at minimum input voltage ($176V_{RMS}$): Output voltage (100 V/div); Line voltage (100V/div); Line current (10 A/div) and switch command.

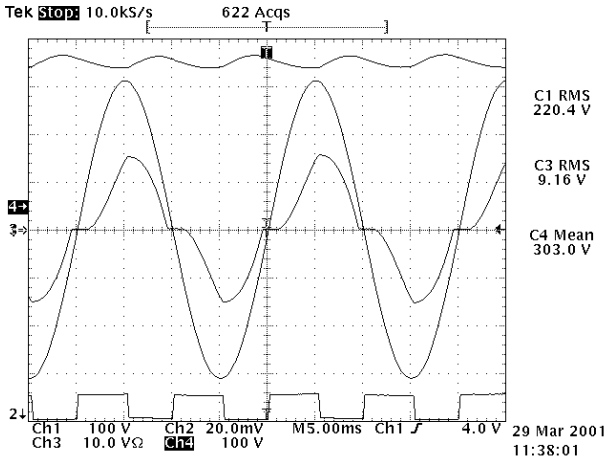

Fig. 6 – Waveforms at nominal input voltage ($220V_{RMS}$): Output voltage (100 V/div); Line voltage (100V/div) and current (10 A/div) and switch command.

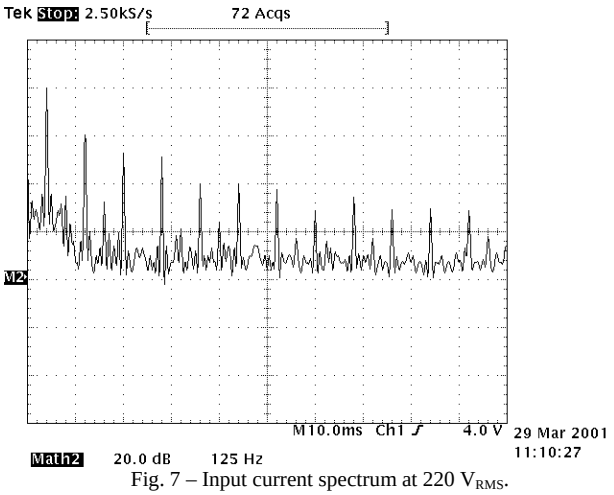

Fig. 7 – Input current spectrum at 220 V_{RMS}.

Table II: Prototype current harmonic components and EN 61000-3-2 limits

I_n	Harmonics [A_{rms}]	Class A limits [A_{rms}]
I_1	9.120	
I_3	2.150	2.300
I_5	0.400	1.140
I_7	0.330	0.770
I_9	0.096	0.400
I_{11}	0.088	0.330
I_{13}	0.064	0.210
I_{15}	0.029	0.150
I_{17}	0.050	0.132
I_{19}	0.028	0.118
I_{21}	0.029	0.107
I_{23}	0.024	0.098

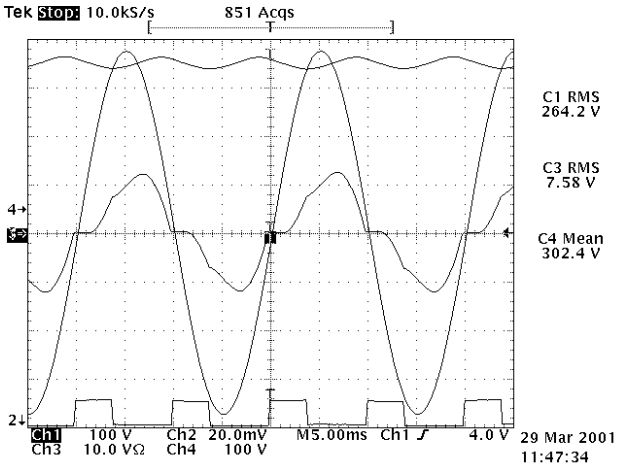

Fig. 8 – Waveforms at maximum input voltage ($264V_{RMS}$): Output voltage (100 V/div); Line voltage (100V/div) and current (10 A/div) and switch command.

Without the auxiliary circuit operation, the resulting waveforms are shown in Fig. 9 for the rated voltage. The output voltage drops to 211 V, thus reducing the output power to 844 W. The efficiency is 93% and the Power Factor is 78 %.

For all the situations the output voltage is lower than the expected due to the non unity converter efficiency.

Comparing the results with and without the auxiliary circuit, it is clear that, without additional losses, it is possible to reduce the current distortion, thus improving the power factor, and to stabilize the output dc voltage in a wide input voltage variation range.

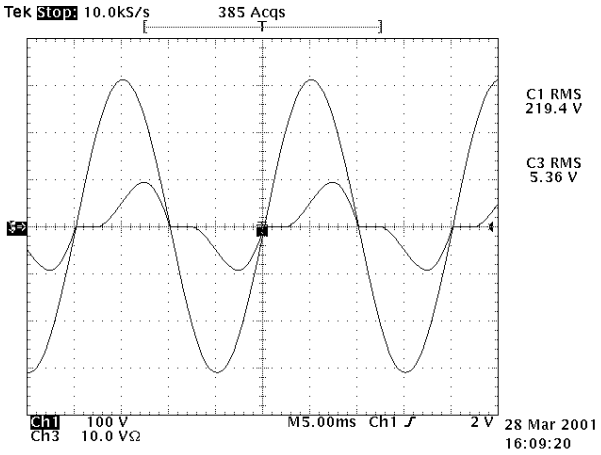

Fig. 9 – Waveforms with passive filter, at rated input voltage ($220V_{RMS}$): Line voltage (100V/div) and current (10 A/div).

V. CONCLUSIONS

The presented add-on line-frequency commutated cell is able to greatly improve both power factor and output voltage regulation of rectifiers with passive L-C filters. The boost action allows for the compensation of the voltage drop across the input filter inductor, so as output voltages higher than the peak of the line voltage can be achieved.

Moreover, as compared to the line-frequency commutated boost rectifier, the proposed circuit allows compliance with the low-frequency harmonic standard EN 61000-3-2 with a lower filter inductance value, at output power levels greater than 1kW.

A converter prototype was built and tested, verifying the expectations.

ACKNOWLEDGMENT

The authors wish to acknowledge the support of FAPESP (Fundação de Amparo à Pesquisa do Estado de São Paulo).

REFERENCES

1. IEC 1000-3-2, First Edition 1995-03, Commission Electrotechnique Internationale, 3, rue de Varembé, Genève, Switzerland.
2. M. Jovanovic, D. E. Crow, "Merits and Limitations of Full-Bridge Rectifier with LC Filter in Meeting IEC 1000-3-2 Harmonic-Limit Specifications," IEEE Applied Power Electronics Conf. Proc. (APEC), March 1996, pp. 354-360.
3. I. Suga, M. Kimata, Y. Ohnishi, R. Uchida, “New Switching Method for Single-Phase AC to DC Converter”, PCC Conf. Proc., Yokohama, 1993, pp. 93-98
4. L. Rossetto, G. Spiazzi, P. Tenti, "Boost PFC with 100Hz Switching Frequency providing Output Voltage Stabilization and Compliance with EMC Standards," IEEE Transaction on Industry Applications, vol.36, n.1, January/February, 2000, pp.188-193.
5. S. Buso, G. Spiazzi, “A Line-Frequency Commutated Rectifier Complying with Standards”, IEEE Applied Power Electronics Conf. Proc. (APEC), March, 1999, pp. 356-362.
6. J. A. Pomilio, G. Spiazzi, “A Double-Line-Frequency Commutated Rectifier Complying with IEC 1000-3-2 Standards”, IEEE Applied Power Electronics Conf. Proc. (APEC), March, 1999, pp. 349-355.